

EFFECT OF GRAPHENE OXIDE ON MECHANICAL, THERMAL AND PHYSICAL PROPERTIES OF IMPACT MODIFIED POLY(LACTIC ACID) NANOCOMPOSITES

Muhammad Amirul Solihin Mazlan¹, Zainoha Zakaria^{1*}, Muhammad Akmal Ahmad Saidi², Azman Hassan², Chan Jia Xin²

¹Department of Chemistry, Faculty of Science, Universiti Teknologi Malaysia, 81310 Johor Bahru, Malaysia

²School of Chemical and Energy Engineering, Faculty of Engineering, Universiti Teknologi Malaysia, 81310 Johor Bahru, Malaysia

* Corresponding author: zainoha@kimia.fs.utm.my

ABSTRACT

The advantage of nanofillers such as graphene oxide (GO) is the ability to improve several properties of polymers at relatively small amount of loadings. The objective of this study is to investigate the effect of GO on mechanical, thermal and physical properties of impact modified polylactic acid (PLA) nanocomposites. The incorporation effect of core shell rubber (CSR) as impact modifier into the PLA and PLA/GO composites is investigated. In this study, the weight ratio of PLA:CSR was fixed at 95:5 wt %. Different GO contents (0, 0.5, 1.0, 2.0 phr) was then incorporated into the PLA/CSR sample. From mechanical properties analysis, it was found that the presence of CSR causes a slight reduction in the flexural properties. The addition of GO enhanced the flexural properties with an increment of 41.6% and 11.9% for flexural strength and modulus respectively. Thermogravimetric analysis showed that CSR decreased the degradation temperature of PLA while GO improved the thermal stability of the nanocomposites. The potential of GO in improving thermal stability of PLA was highlighted by the glass transition temperature and melting temperature shifting to a higher temperature. Physical properties were analyzed by soil burial degradation test and water absorption test. Soil burial test showed insignificant changes of weight loss as compared during the initial burial period. The water absorption test is at 30°C and 50°C immersion temperature. At 30°C, the results highlighted the superior effect of GO due to its hydrophilic properties. At higher temperature, the amount of water absorbed by PLA and its nanocomposites was higher due to swelling structure of PLA. The results of soil degradation showed that PLA has slow degradation in soil. In conclusion, incorporation of GO at low content into impact modified PLA showed appreciable improvement in the mechanical, physical, and thermal properties of impact modified PLA. This study contributes to the development of advanced bio-based composites.

Keywords: *graphene oxide; poly(lactic acid); flexural properties; thermal properties; water absorption*

1.0 INTRODUCTION

In recent years, plastics obtained from petrochemical sources is not the primary option in daily usages anymore. Society began to realize the importance of choosing biopolymer material in their products for the benefit of future generations. The development of biodegradable polymers from natural resources has provided an excellent alternative for society to reduce their dependency on petroleum-based plastics [1].

Poly(lactic acid) (PLA) is a polyester made of renewable raw materials with linear aliphatic thermoplastic properties. It is a synthetic polymer made from lactic acid as its monomer which typically a bioproduct from bacterial fermentation of agricultural substrate such as corn, sugarcane or cassava. Nowadays, PLA becomes popular in most of the polymer products due to its biocompatibility, sustainability and compostable properties that makes it non-toxic to the environment. However, these versatile applications of PLA products found to be limited as it is found to have brittle character in thicker materials, have lower thermal stability, and when compared to petroleum-derived polymers such as polypropylene and polyethylene, it is also more expensive. Increasing production by many industries globally were believed could change the state of price of the PLA in the future. Modifications and improvements were suggested in order to overcome PLA's mechanicals and thermal limitations so that more applications of PLA can be applied in a larger field of area. There are two approaches which have been found that can be applied to improve the properties of PLA, which is addition of fillers (micro- and nano-) and thermoplastic blending [2].

Graphene Oxide (GO) has been well known for its excellent potential as nanofillers. The presence of GO contributed to the developments of new polymer nanocomposites with great properties in terms of electrical, mechanical, thermal and barrier properties. Compared to graphene, GO has hydrophilic properties that can make it to have strong physical interactions with polymers. The existence of various oxygen functional groups such as carbonyls, carboxyls, epoxide and hydroxyls are the reasons GO can be readily exfoliated in water to yield stable dispersions consisting mostly of single layer sheets, which are referred to GO sheets [3]. On the other hand, addition of impact modifier such as acrylic core-shell rubber (CSR), acrylic rubber (AR), silicone rubber (SI) and synthetic polyisoprene rubber (IR) will further improved PLA composites for wider range of applications. Between these several types of impact modifier, CSR was selected in this study. This is due to their interesting performance that possessed a highest tensile and impact toughness with high percentage of crystallinity when compared to the others as was found from a study by Phattarateera and Pattamaprom [4]. The effect of CSR on the flexural, thermal and physical properties of PLA were also reported in previous study [5].

From the literature, studies which incorporate both GO and CSR together into PLA matrix system are scarce. Hence, the objective of this study is to investigate the effect of adding GO into PLA/CSR matrix which is mixed by melt-blending method. Flexural, thermal and physical properties of PLA/CSR/GO nanocomposites will be studied.

2.0 METHODOLOGY

2.1 Materials

A commercially available polylactide (PLA) (NatureWorks, PLA 3001D) with a melt flow index (MFI) range from 10 to 30 g/10 min (190 °C, 2.16 kg) and a density of 1.24 g/cm³, was purchased from NatureWorks LLC. United Graphene Oxide (UGOXTM) (Graphite Generated Nano Materials) powder (purity: 99%), was supplied by United Nanotech Innovations Private Limited, India, with average thickness of 0.8 to 2.0 nm, average number of 3 to 6 layers and lateral dimension of 5 to 10 µm. CSR (PARALOID EXL-2330) with melting point range of 132-149°C which act as impact modifier and impact modifier was obtained from Rohm and Haas (Philadelphia, Pennsylvania, USA).

2.2 Preparation of Nanocomposites

PLA and CSR were dried for 24 h at 50°C in a vacuum oven to remove moisture before the mixing and extrusion process. PLA, CSR and GO were melt-blended using a Werner & Pfleiderer ZSK25 (Germany) twin screw extruder (L/D = 36) with rotation speed of 40-50 rpm and mixing temperature setting at 190°C. For PLA/CSR/GO nanocomposites preparation, the amount of GO was varied (0, 0.5, 1, 1.5 and 2 phr). The composition of CSR was kept constant at 5 wt % for all nanocomposite formulations. Neat PLA was also extruded as control. The summary of the polymer nanocomposites formulation is tabulated in Table 1. All the extruded samples pelletized and compression molded using a hot press before being cut into test specimens for mechanical testing, thermal and physical analysis.

Table 1 Preparation of PLA/CSR/GO composites formulation.

Sample Formulations	PLA (wt %)	CSR (wt %)	GO (phr)
PLA	100	-	-
PLA/CSR/GO(0)	95	5	-
PLA/CSR/GO(0.5)	95	5	0.5
PLA/CSR/GO(1.0)	95	5	1.0
PLA/CSR/GO(1.5)	95	5	1.5
PLA/CSR/GO(2.0)	95	5	2.0

2.3 Sample Analysis

2.3.1 Mechanical Properties

Evaluation on the effect of different GO contents to the mechanical properties of PLA nanocomposites was done by flexural test according to ASTM D790. The flexural test was carried out via Lloyd testing machine (West Sussex, United Kingdom) with 20 kN load, 2 mm min⁻¹ testing speed and support span of 45 mm, under ambient conditions. Five specimens of each formulation were used for which the average value was reported.

2.3.2 Thermal Properties

2.3.2.1 Thermogravimetric Analysis

Using thermogravimetric analysis (TGA), the amount of mass loss of the PLA/CSR/GO composites during heating were analyzed. The thermal stabilities of the nanocomposites were investigated using TGA/DTG, TA instrument (Model: TGA Q500) with alumina crucible using 10 mg of sample as probe. Analysis started at ambient temperature to 600°C with heating rate of 10°C min⁻¹ under nitrogen atmosphere.

2.3.2.2 Differential Scanning Calorimetry

The melting and crystallization behavior of the blends and the nanocomposite were investigated using Perkin-Elmer DSC-6 differential scanning calorimeter (DSC). Prior to that, all samples were weighed to approximately 10 mg and sealed into aluminium pans. The samples were heated from 20°C to 250°C at a heating rate 10°C min⁻¹. The analysis revealed the glass transition (T_g), melting behavior (T_m) and crystallization of the nanocomposites. The degree of crystallinity, X_c (%) of PLA blend and its nanocomposites were calculated using Equation 1.

$$X_c = \frac{\Delta H_m - \Delta H_{cc}}{\Delta H_m^0 \times \phi} \times 100\% \quad (1)$$

where ΔH_m is the fusion enthalpy of PLA measured from DSC analysis, ΔH_c is the cold crystallization enthalpy, ϕ is the weight fraction of PLA in the sample and ΔH_m^0 is the fusion enthalpy of PLA at 100% crystallinity selected as 93 J g⁻¹ [6].

2.3.3 Characterization

2.3.3.1 Attenuated Total Reflectance-Fourier Transform Infrared Spectroscopy

The chemical compositions of PLA/CSR/GO with different GO content were recorded by attenuated total reflectance-Fourier transform infrared spectroscopy (ATR-FTIR), on a Perkin Elmer FTIR spectrometer. The spectra were recorded in the range from 400 to 4000 cm⁻¹. Characterizations were done to observe the interactions that may happen in the composites.

2.3.4 Physical Properties

2.3.4.1 Soil Burial Test

Soil burial test was conducted with the purpose of studying biodegradation of composites in natural conditions using garden soil [7]. The garden soil used contained a balance of three soil materials namely silt, sand and clay with humus. It has a pH of 6-6.5 and high calcium levels

because of its previous organic matter content. Rectangular samples (150 x 150 x 15 mm dimension) were kept in a desiccator until a constant weight (W_1) was achieved. The samples were then buried in garden soil at a depth of 170-220 mm from the soil surface for durations of 17 weeks. The soils were sprayed with water every 24 hours to maintain its moisture. After burying at selected durations, samples were then washed with water to remove the soil from the surface of samples and dried at 55°C in oven and kept in desiccator until it reached a constant weight (W_2). The percentage of weight loss (%WL) was calculated according to Equation 2.

$$\%WL = \left[\left(\frac{W_1 - W_2}{W_1} \right) \times 100\% \right] \quad (2)$$

2.3.4.2 Water Absorption Test

The specimens (dimension: 150mm x 150mm x 15mm) were dried at 50°C in vacuum oven until a constant weight was reached. Samples were then immersed in water in a thermostatic stainless-steel water bath at 30, and 50°C for 14 days. Weight changes were recorded by periodic removal of the specimens from the water bath and weighing on a balance with a precision of 1 mg. The percentage change at any time t , (M_t) as a result of water absorption was determined by Equation 3.

$$M_t = \frac{W_w - W_d}{W_d} \times 100\% \quad (3)$$

where, W_d and W_w denote the weight of dry material (the initial weight) and average weight of materials after exposure to water absorption, respectively.

3.0 RESULTS AND DISCUSSION

3.1 Flexural Properties

The effects of CSR on the flexural strength and modulus of PLA blends were investigated, and the results are shown in Figure 1. It can be seen that the strength and modulus of the blend has reduced by about 14.70% and 8.17% respectively as compared to neat PLA. The flexural strength of the blends reduced to 15.10 MPa and its modulus decreased to 1808.62 MPa. These results follow early expectations and agreed with the previous work [7]. The work of Petchwattana and Covavisaruch described that CSR softened the PLA/CSR blends softened when compared to neat PLA under bending force. Microscopic observation was employed by them using scanning electron microscope (SEM) to observe the fracture morphology of the blends. The results obtained confirming that the fracture surfaces of the PLA blends showed more localized plastic deformations with the present of CSR content. The localization of plastic deformation into a shear band was discussed as an instability of plastic flow and a precursor to rupture.

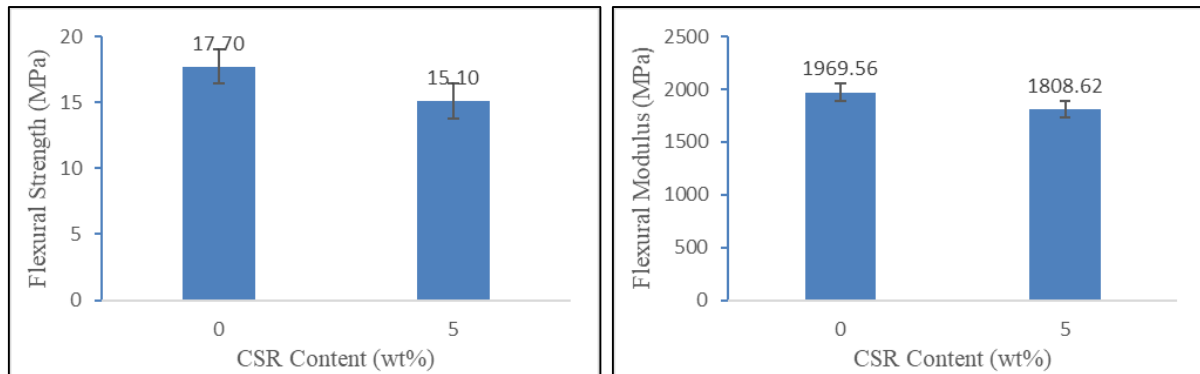


Figure 1 Effect of CSR on flexural properties of PLA.

Figure 2 shows the effects of different GO contents on the flexural properties of PLA/CSR. It can be seen that both flexural strength and modulus show the same trend in which they have an initial increase at the beginning of incorporations of GO and reaching a maximum at 1.5 phr of GO contents. When comparing between PLA/CSR and the highest flexural properties reached at 1.5 phr of GO loadings, the increments represented 41.63% and 11.93% of changes for flexural strength and modulus respectively. The results are owing to the excellent properties of GO, including greater surface area, surface roughness and polarity which make GO form stronger intermolecular interactions with the polymer matrix [8]. Yet, the beneficial effect from GO will be reduced when the GO content exceeds the optimal value due to the agglomeration of GO in composites, which reduces the active reaction sites on GO to form bonding [9]. The great improvement in flexural properties of PLA/CSR/GO nanocomposites suggested its potential applications in construction sector such as plastic lock arm, snap fit assemblies or diving board.

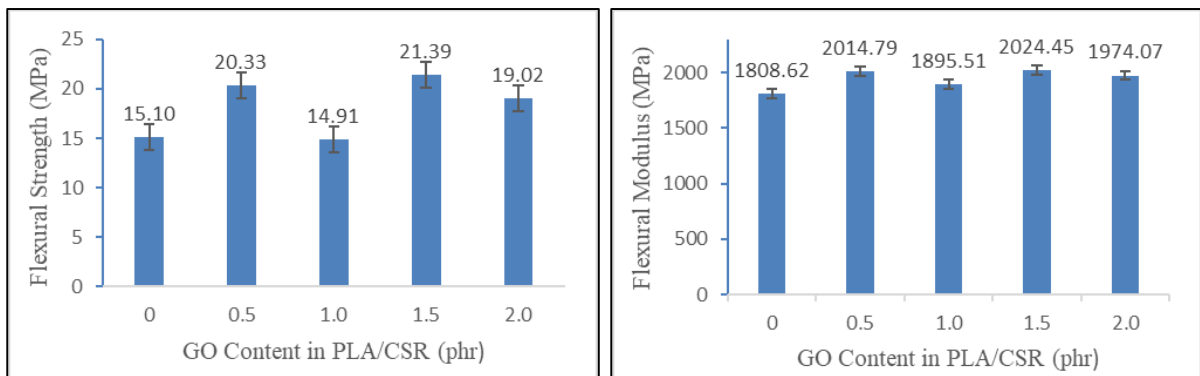


Figure 2 Effect of GO contents on flexural properties of PLA/CSR.

Low values of flexural strength at 1.0 phr of GO incorporations were due to the formation of air cavities as shown in Figure 3 (a). As a comparison, Figure 3 (b) shows the broken samples of the other formulations without any voids. The air cavities in the samples were formed during the compression molding process and can affect the mechanical strength of the sample.

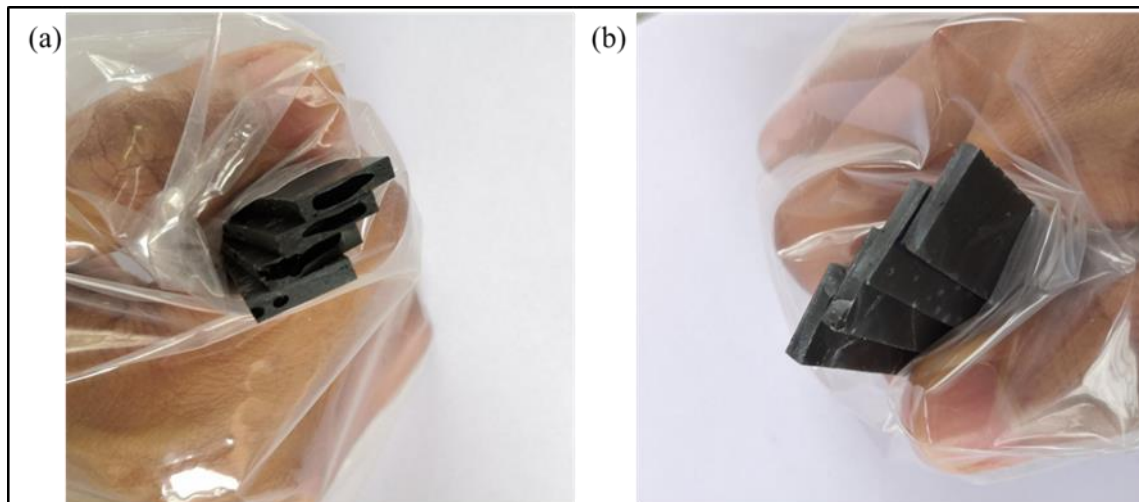


Figure 3 Broken sample after flexural test a) Presence of air cavities b) Perfect mold.

Ductility is a measure of a material's ability to undergo significant plastic deformation before rupture or breaking. In this study, strain can be observed as an indication of the polymer's ductility. Note that, the strain at maximum stress measured throughout this study is also the strain in which the sample break, strain at break. As shown in Figure 4, it is observable that the effect of CSR as impact modifier is not effective in improving the ductility of PLA. Possible reason for this behavior is because the condition in which this flexure test being run is at low strain rate, 2 mm min^{-1} . However, at higher strain rate condition such as in impact test, there is a strong possibility that the impact strength will increase. This is supported by the previous work on PLA/CSR [4]. Further studies are needed to study the effect of the CSR to the PLA's impact strength. Increasing strain pattern in which GO incorporations is introduced also needed a more attentive study to explain the real reason behind their behaviors.

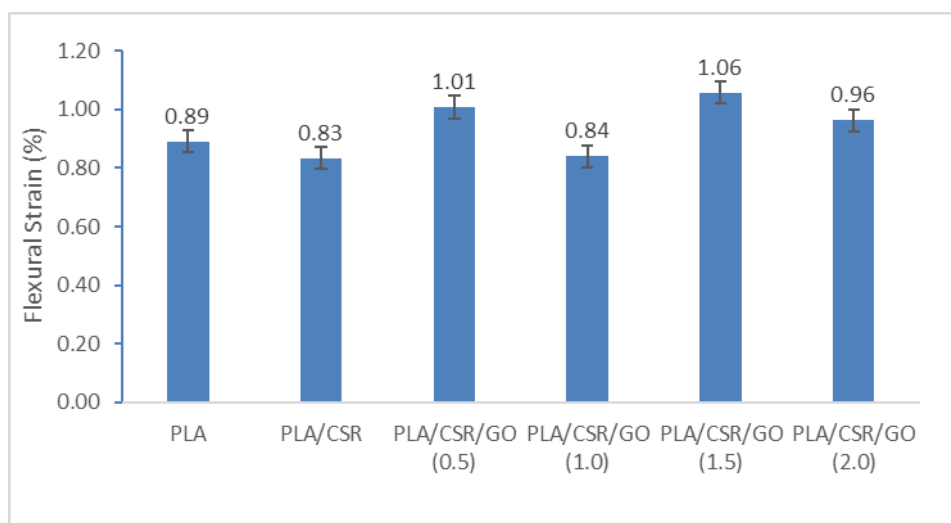


Figure 4 Flexural Strain of PLA and its composites.

3.2 Thermogravimetric Analysis

Figures 5 and 6 show the TGA thermograms and derivative thermogram (DTG) for PLA/CSR nanocomposites at different loading of GO. Table 2 provides the detailed data on char residue and temperatures at mass loss of 10% ($T_{10\%}$) and during maximum degradation peak (T_{peak}) of the DTG. Neat PLA shows a complete degradation at 370°C with 0% residue left. Apparently, all PLA/CSR/GO nanocomposites exhibit higher char residue at 600°C than the neat PLA. The high char residue remains at high temperature in TGA analysis is made of carbon materials that cannot be further dissociated into smaller volatile fragments. Therefore, even there is a slight decrease at 0.5 phr, it is quite obvious that there is increasing trend of char residue in PLA/CSR/GO with the increase content of GO as it is representing the amount of GO phase in the nanocomposite. Presence of CSR is represented by the higher amount of char residue in PLA/CSR compared to neat PLA.

PLA/CSR shows a lower degradation temperature as compared to neat PLA in thermal degradation at $T_{10\%}$ and T_{peak} . CSR is concluded can strongly influence in lowering the thermal stability of PLA. After incorporation of GO, the degradation temperature of the PLA/CSR/GO nanocomposite (Table 2) at $T_{10\%}$ shows a shifting to a higher temperature as compared with PLA/CSR blend starting at 0.5 phr of GO loading. These shifts could be explained due to the interfacial interactions existed between GO and PLA through hydrogen bonds and/or van der Waals forces [10]. However, the inclination still could not pass the higher value of thermal degradation that the neat PLA possessed. The only possible reason for this outcome is mainly due to the presence of CSR in all PLA/CSR/GO which lowered the thermal stability of the nanocomposite. Further addition of GO loadings to 2.0 phr led to a shifting of thermal degradation temperature to a lower temperature as shown in Table 1 for both $T_{10\%}$ and T_{peak} . This indicates that agglomeration of GO has occurred which caused a decrease in the thermal stability PLA/CSR/GO composites.

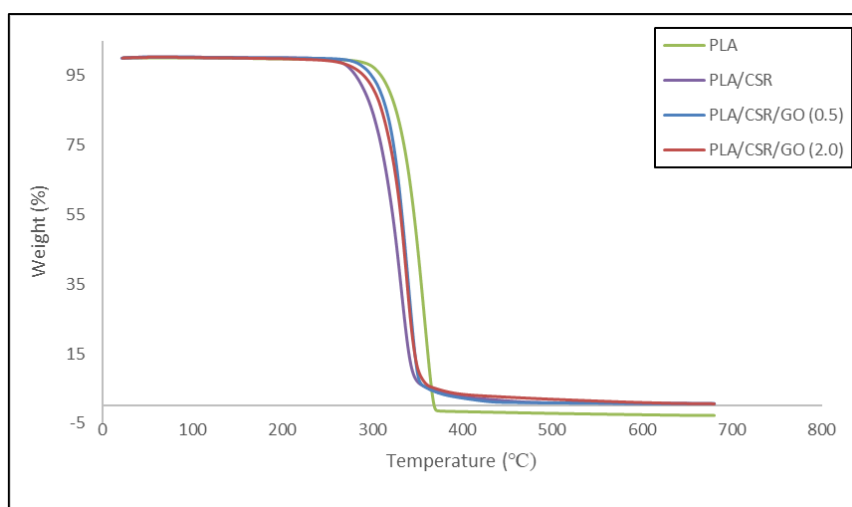


Figure 5 TGA thermograms of PLA, PLA/CSR and PLA/CSR/GO of 0.5 and 2.0 phr.

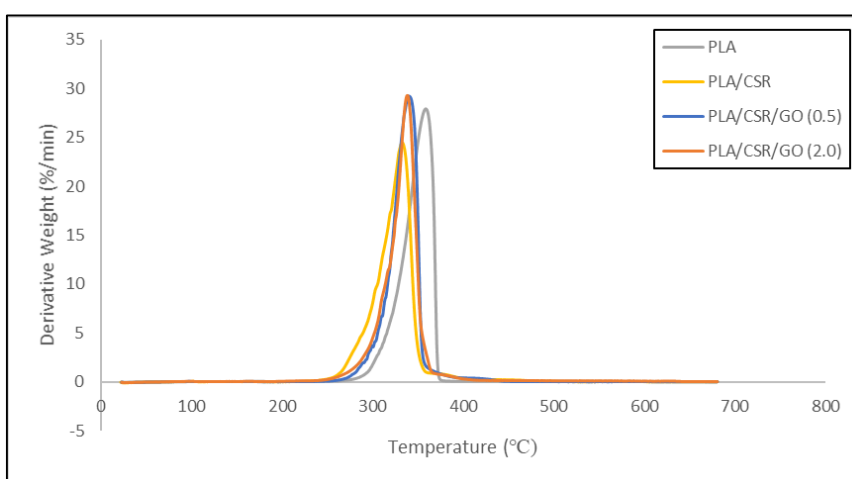


Figure 6 DTG thermograms of PLA, PLA/CSR and PLA/CSR/GO of 0.5 and 2.0 phr.

Table 2 Thermogravimetric Analysis data of PLA, PLA/CSR and its nanocomposites.

Sample	Degradation Temperature (°C)		Char residue at 600°C (%)
	T _{10%}	T _{peak}	
PLA	320	358.6	0
PLA/CSR	292.4	332.3	0.69
PLA/CSR/GO (0.5 phr)	309.6	340.0	0.66
PLA/CSR/GO (2.0 phr)	303.4	338.2	0.95

3.3 Differential Scanning Calorimetry

The DSC thermogram curves and its analyzed data of PLA, PLA/CSR blends and PLA/CSR/GO composites are compared and shown in Figure 7 and Table 3, respectively. Note that the cold crystallization temperature (T_{cc}) could not be measured accurately indicating maximum crystallinity level. The unprocessed PLA pellet also showed no measurable T_g due to high crystalline content of the samples as it reached 44% for X_c . The effect of CSR loadings in neat PLA can only be compared from the difference in crystalline T_m . It was found that T_m for all PLA/CSR blends seemed to be slightly higher than of neat PLA implying that the addition of CSR might assist in forming more perfect crystals [4].

The T_g value of the nanocomposites increased and reached maximum value of 62.54 °C at 0.5 phr of GO loadings. These results support a study by Liao *et al.* [11] which stated that the T_g of graphene and GO/polymer nanocomposites will significantly increase (4°C or more) when using functionalized nanofillers, due to more interactions with the matrix. They explained that blending processes, such as solvent and melt blending which do not involve covalent bonding to the graphene surface, are generally incapable of providing enough restriction by interactions between the matrix polymers and fillers. However, the chains of polar polymers with low T_g can be confined by strong hydrogen bonding to graphene containing oxygen groups such as thermally reduced graphene (TRG), chemically reduced graphene (CRG), and GO. Due to that, they typically show an increase in T_g . Degree of crystallinity increased and maximized at 1.0 phr, then decreased as the GO is further added. It may be due to the effect of GO agglomeration [12].

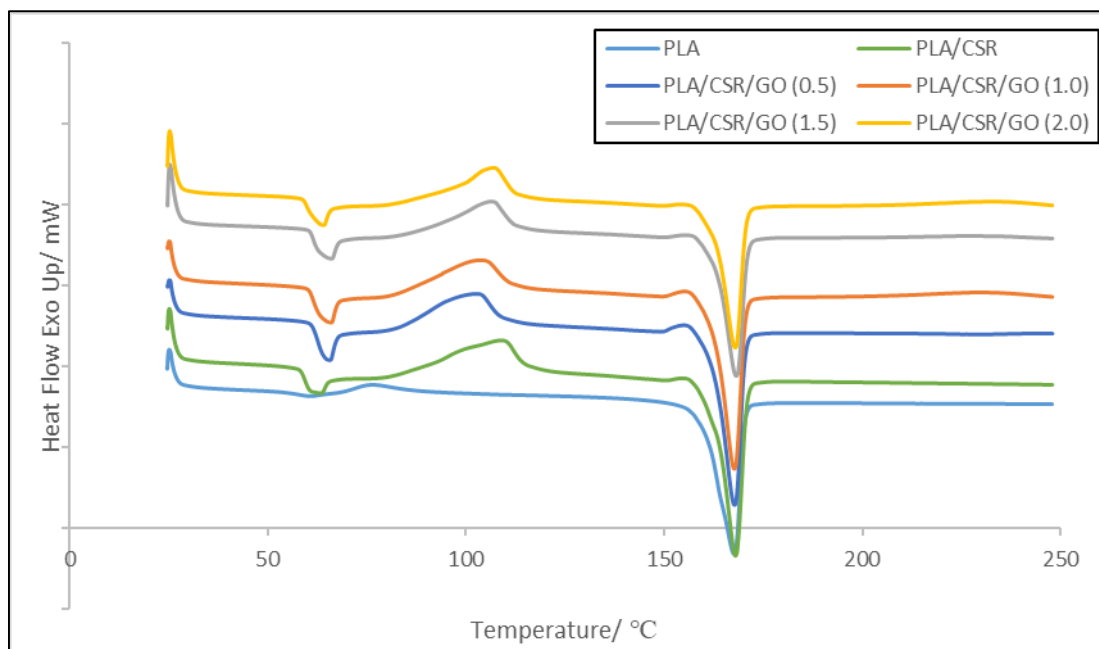


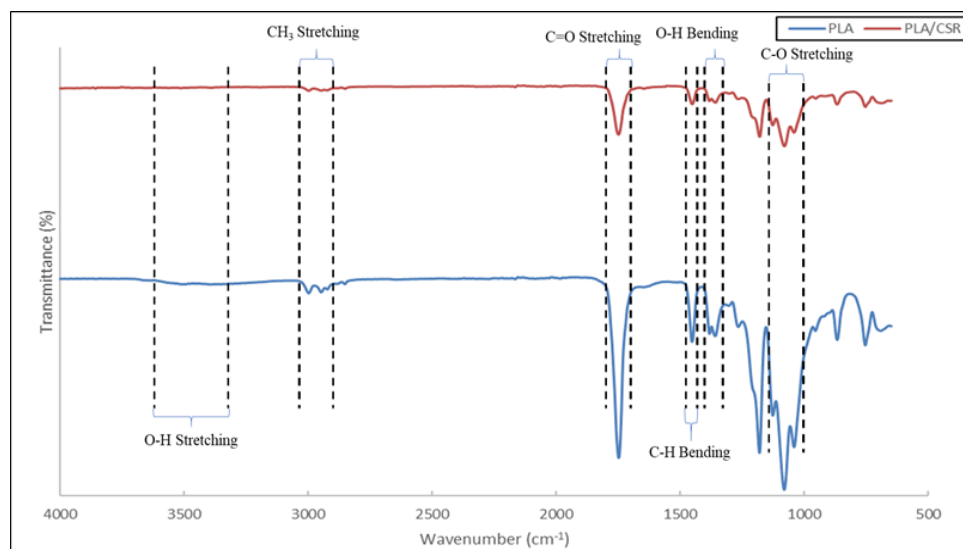
Figure 7 DSC thermograms of PLA, PLA/CSR and PLA/CSR/GO of 0.5, 1.0, 1.5 and 2.0 phr.

Table 3 DSC thermal data of neat PLA, PLA/CSR and PLA/CSR/GO nanocomposites.

Sample	T_g (°C)	T_m (°C)	T_{cc} (°C)	ΔH_m (Jg ⁻¹)	ΔH_c (Jg ⁻¹)	X_c (%)
PLA	n/a	167.7	n/a	43.896	n/a	43.72
PLA/CSR	59.64	168	108.77	47.065	29.942	19.38
PLA/CSR/GO (0.5)	62.54	167.76	102.53	40.681	20.318	23.05
PLA/CSR/GO (1.0)	62.08	167.71	103.69	41.576	19.257	25.26
PLA/CSR/GO (1.5)	62.16	168.22	106.6	35.824	15.214	23.33
PLA/CSR/GO (2.0)	60.63	167.95	106.84	35.478	17.151	20.74

3.4 Attenuated Total Reflectance-Fourier Transform Infrared Spectroscopy

Figure 8 shows the IR spectrum of the PLA and PLA/CSR composite at different GO content. The spectrums exhibit CH₃ stretching (2900-3000 cm⁻¹) with four peaks in each formulation which presumably represent the CH₃ bonding of the PLA. Also, in all formulations, a sharp C=O stretching peak presence at ~1750 cm⁻¹ and C-O-C stretching peak at ~1180 cm⁻¹ characterize the presence of ester bonds in PLA. It can be seen that the O-H bond of PLA is still present at ~3400 cm⁻¹ region but at lower transmittance. This results presumably due to low amount of terminal hydroxyl group present at the surface of the PLA. Incorporation of GO into the PLA and PLA/CSR blends showing some increase in O-H group peak indicates the presence of GO which have abundance of oxygen-containing functional groups on its surface [13].



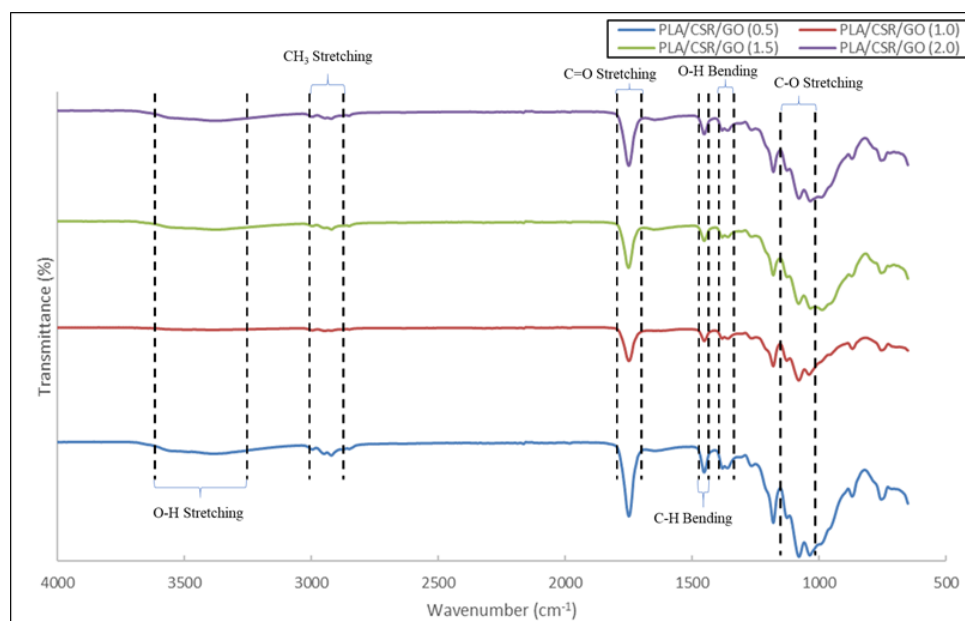


Figure 8 FTIR spectra of neat PLA, PLA/CSR and PLA/CSR/GO nanocomposites.

Interestingly, the FTIR spectra of PLA/CSR blend show the absence of O-H bond which indicates the occurrence of interaction between PLA and CSR. It is deduced that the PMMA shell of CSR is responsible for the observed physical interaction with PLA. The possible interaction between PMMA and PLA might occur through dipolar interaction between the ester groups of both polymers due to difference polarity exhibited by the ester groups.

3.5 Soil Burial Test

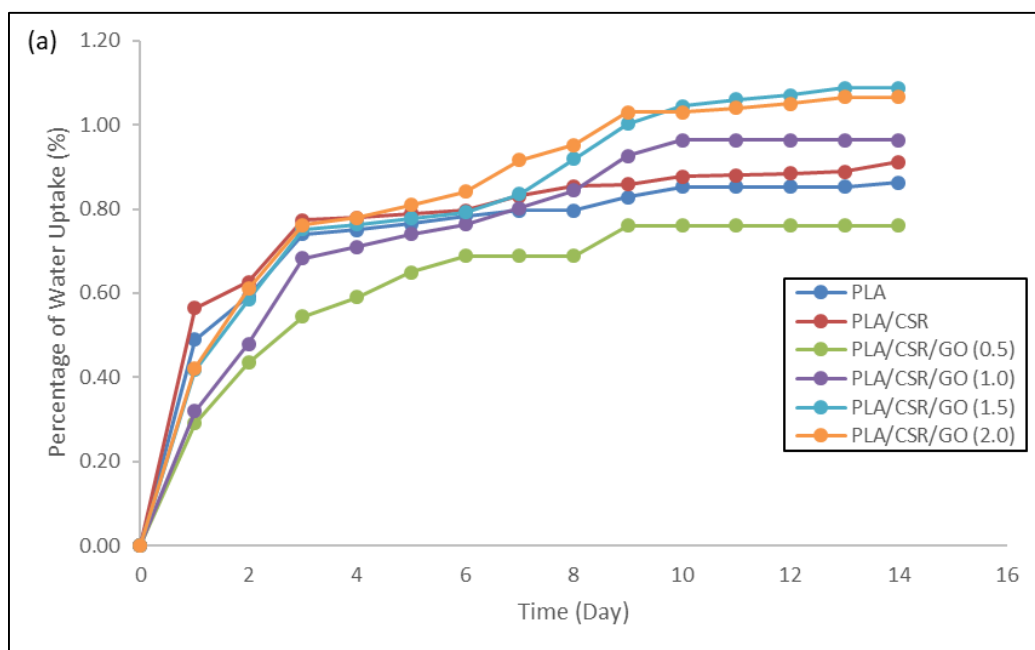
The biodegradability of PLA, PLA/CSR, PLA/CSR/GO of 0.5, 1.0, 1.5 and 2.0 phr were conducted using soil burial test. The weight loss of PLA, PLA/CSR blends and PLA/CSR/GO composites are shown in Table 4. Overall, after 17 weeks being buried in soil, the amount of PLA being degraded is relatively very small (~0.1%). Compared to previous research [14], this result confirms that PLA possessed the properties of slow degradation in soil and takes long time for the degradation to start. Even after the incorporation of CSR and GO, the changes difference between the formulations are still considered insignificant. This is most probably due to its slow rate of hydrolysis at low temperatures and water contents and the relative scarcity of PLA degrading organisms [14]. PLA requires a composting environment (45-60 days at 50-60 °C) which can promote hydrolyzation into smaller molecules (oligomers, dimers and monomers) followed by degradation into CO₂ and H₂O by microorganisms within the compost [15].

Table 4 Weight loss of PLA nanocomposites.

Sample	Weight loss (%)
PLA	0.11
PLA/CSR	0.11
PLA/CSR/GO (0.5)	0.11
PLA/CSR/GO (1.0)	0.13
PLA/CSR/GO (1.5)	0.13
PLA/CSR/GO (2.0)	0.12

3.6 Water Absorption Test

Water absorption tests of PLA, PLA/CSR and PLA/CSR/GO with various GO loadings were done at two different immersion temperatures of 30°C and 50°C as illustrated in Figure 9 (a) and (b) respectively. The final water uptake at both immersion temperatures is shown in Table 5. All results show a rapid increase at initial period of immersion in the water and before coming to a steady state after a period of time. PLA/CSR shows a higher amount of water absorption than the neat PLA after 2 weeks at both temperatures. PLA only absorb 0.86 % and 2.09 % in 30°C and 50°C temperature of water respectively, while PLA/CSR could reach to 0.91 % and 2.47 % in 30 and 50°C conditions, respectively. This indicates that the presence of CSR has improved the hydrophilicity behavior of the PLA. This can be related with the presence of hard-shell presence in CSR named styrene-acrylonitrile (SAN). It is known to be hygroscopic polymer and it has been reported can absorb up to 0.4% of moisture. In addition, there is also a tendency for the acrylate rubber forming the core of the CSR to absorb moisture because polyacrylates are also known to be a hygroscopic material [16].



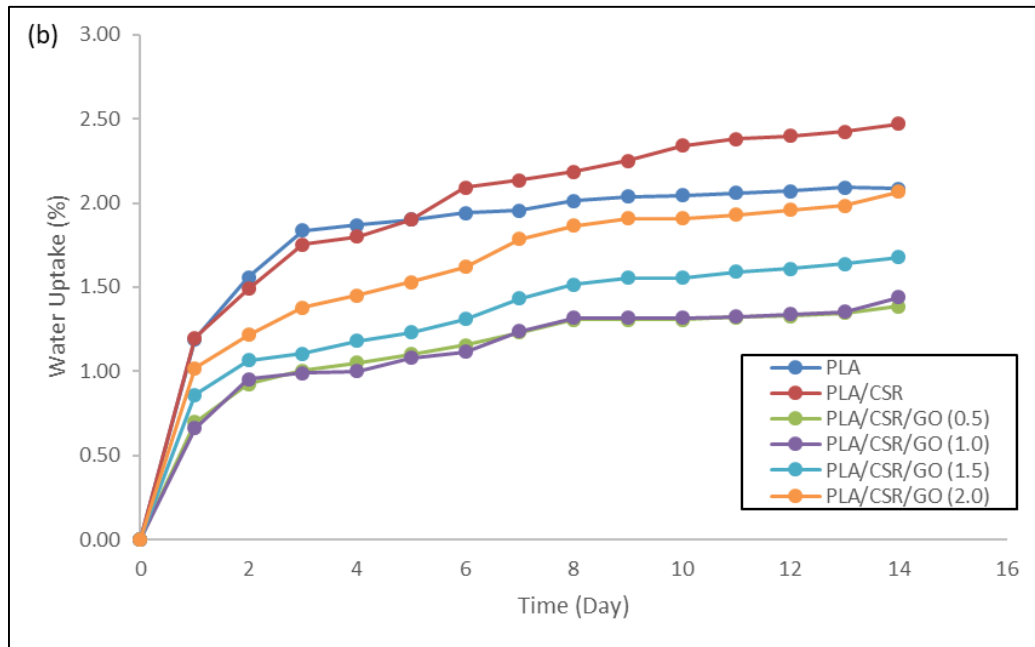


Figure 9 Water absorption of PLA and its composites at immersion temperature of (a) 30°C (b) 50°C.

At 30°C immersion temperature (Figure 9a), the absorption of water shown by the nanocomposites with the presence of GO is higher compared to PLA. Highest water absorption is when the incorporation of GO is at 1.5 phr. The results obtained correlate with the properties of GO found from previous study [17]. It is known that functional groups in the GO structure open gaps between the stacked platelets that are approximately 1 nm wide. These gaps in GO provide channels for transportation and storage of water molecules. In addition, these hydrophilic groups can adsorb and retain water molecules forming hydrogen bonds. Water molecules are adsorbed physically by being trapped inside capillaries or on the surface, yet their chemical properties remain unchanged. In Figure 9(b), it can be seen that the PLA have a dramatic increase compared to other composites at the initial of immersion period. The addition of GO and CSR might had delayed the absorption. As observed in Figure 9(b) it can be seen that the saturation time of PLA was achieved after 8 days upon subjected to hygrothermal aging at 50°C. Overall, the amount of water absorbed by PLA and its nanocomposites is higher when the temperature is raised to a higher temperature as shown in Figure 10. The higher temperature has caused an increase in swelling structure of PLA. This subsequently induces higher water absorption.

Table 5 Effect of temperature to the water absorption of PLA and its composites.

Sample Designation	Water Uptake (%)	
	30°C	50°C
PLA	0.86	2.09
PLA/CSR	0.91	2.47
PLA/CSR/GO (0.5)	0.76	1.39
PLA/CSR/GO (1.0)	0.96	1.44
PLA/CSR/GO (1.5)	1.09	1.68
PLA/CSR/GO (2.0)	1.07	2.07

4.0 CONCLUSION

For mechanical properties, loadings of CSR into neat PLA has caused a reduction in the flexural strength, modulus and strain due to localized plastic deformations at the fractured blends surface induced by the CSR. Optimum amount of GO incorporations for the maximum GO dispersion in PLA/CSR blends is found to be at 1.5 phr as it contributes to the highest improvement in flexural properties of the composites. Further incorporations of GO loading has led to a decrease in flexural properties probably due to agglomeration that might start to happen. CSR as impact modifier show ineffective result to the composites and the low strain rate might be the reason for its behavior. Impact test at higher strain rate might show a different outcome. In thermal analysis by TGA, presence of CSR has shifted $T_{10\%}$ and T_{peak} to a lower degradation temperature. While the incorporations of GO loadings has led to an improvement of the thermal stability of the PLA as the thermal degradation is shifted to a higher temperature. The improvement is due to interfacial interactions existed between GO and PLA through hydrogen bonds and/or van der Waals forces. DSC results also show a positive impact of GO to the PLA matrix as the T_g changed to a higher temperature. FTIR analysis was done to observe some interactions that might have occurred. Incorporation of GO into the PLA and PLA/CSR blends showing some increase in O-H group peak indicates the presence of GO which have abundance of oxygen-containing functional groups on its surface. Absence of O-H bond when CSR is early introduced without GO is due to the interactions between PMMA shell of CSR with the PLA. The results of soil degradation show insignificant changes of weight loss as compared during the initial burial period. This is mainly due to PLA properties which possessed slow degradation in soil. In conclusion, it needs composting environment for it to be hydrolyzed into oligomers, dimers and monomers. PLA nanocomposites showed different water absorption behavior at 30 and 50°C immersion temperature. At 30°C immersion temperature, PLA with the presence of GO show a superior absorption property due to hydrophilic properties possessed by GO. At 50°C, the amount of water absorbed by PLA and its nanocomposites is higher when the temperature is increased to a higher temperature due to swelling structure of PLA which is influenced by high temperature.

Acknowledgement

The authors would like to express their appreciation to Faculty of Science and Faculty of Engineering, Universiti Teknologi Malaysia for providing the facilities and equipment.

REFERENCES

- [1] Awal, A., Rana, M., & Sain, M. (2015). Thermorheological and mechanical properties of cellulose reinforced PLA bio-composites. *Mechanics of Materials*, 80, 87-95.
- [2] Balakrishnan, H., Hassan, A., & Wahit, M. U. (2010). Mechanical, thermal, and morphological properties of polylactic acid/linear low-density polyethylene blends. *Journal of Elastomers & Plastics*, 42(3), 223-239.
- [3] Xu, Y., Bai, H., Lu, G., Li, C., & Shi, G. (2008). Flexible graphene films via the filtration of water-soluble noncovalent functionalized graphene sheets. *Journal of the American Chemical Society*, 130(18), 5856-5857.
- [4] Phattarateera, S., & Pattamaprom, C. (2019). Comparative performance of functional rubbers on toughness and thermal property improvement of polylactic acid. *Materials Today Communications*, 19, 374-382.
- [5] Tee, A. H., Zakaria, Z., Hassan, A. & Saidi, M. A. A. (2020). Effect of halloysite nanotube on the mechanical, physical and thermal properties of impact modified poly(lactic acid). *PERINTIS eJournal*, 10(1), 50-68.
- [6] Shi, Y., Li, Y., Wu, J., Huang, T., Chen, C., Peng, Y., & Wang, Y. (2011). Toughening of poly (L-lactide)/multiwalled carbon nanotubes nanocomposite with ethylene-co-vinyl acetate. *Journal of Polymer Science Part B: Polymer Physics*, 49(4), 267-276.
- [7] Petchwattana, N., & Covavisaruch, S. (2014). Mechanical and morphological properties of wood plastic biocomposites prepared from toughened poly (lactic acid) and rubber wood sawdust (*Hevea brasiliensis*). *Journal of Bionic Engineering*, 11(4), 630-637.
- [8] Gómez-Navarro, C., Burghard, M., & Kern, K. (2008). Elastic properties of chemically derived single graphene sheets. *Nano letters*, 8(7), 2045-2049.
- [9] Kang, W.-S., Rhee, K. Y., & Park, S.-J. (2017). Influence of surface energetics of graphene oxide on fracture toughness of epoxy nanocomposites. *Composites Part B: Engineering*, 114, 175-183.
- [10] Villar-Rodil, S., Paredes, J. I., Martínez-Alonso, A., & Tascón, J. M. (2009). Preparation of graphene dispersions and graphene-polymer composites in organic media. *Journal of Materials Chemistry*, 19(22), 3591-3593.
- [11] Liao, K.-H., Aoyama, S., Abdala, A. A., & Macosko, C. (2014). Does graphene change T_g of nanocomposites? *Macromolecules*, 47(23), 8311-8319.

- [12] Kuang, T. R., Mi, H. Y., Fu, D. J., Jing, X., Chen, B. y., Mou, W. J., & Peng, X.-F. (2015). Fabrication of poly (lactic acid)/graphene oxide foams with highly oriented and elongated cell structure via unidirectional foaming using supercritical carbon dioxide. *Industrial & Engineering Chemistry Research*, 54(2), 758-768.
- [13] Luo, L., Peng, T., Yuan, M., Sun, H., Dai, S., & Wang, L. (2018). Preparation of graphite oxide containing different oxygen-containing functional groups and the study of ammonia gas sensitivity. *Sensors*, 18(11), 3745.
- [14] Tokiwa, Y., & Calabia, B. P. (2006). Biodegradability and biodegradation of poly(lactide). *Applied Microbiology and Biotechnology*, 72(2), 244-251.
- [15] Pranamuda, H., Tokiwa, Y., & Tanaka, H. (1997). Polylactide Degradation by an *amycolatopsis* sp. *Applied and Environmental Microbiology*, 63(4), 1637-1640.
- [16] Mohd Ishak, Z., Ishiaku, U., & Karger-Kocsis, J. (1999). Hygrothermal aging and fracture behavior of styrene-acrylonitrile/acrylate-based core-shell rubber toughened poly (butylene terephthalate). *Journal of Applied Polymer Science*, 74(10), 2470-2481
- [17] Liu, R., Gong, T., Zhang, K., & Lee, C. (2017). Graphene oxide papers with high water adsorption capacity for air dehumidification. *Scientific Reports*, 7(1), 1-9.